

PROPOSED PROPERTY 2R COUNTEREXAMPLES CLASSIFIED

MARTIN SCHARLEMANN

ABSTRACT. [GST] classified, via a natural slope indexed by \mathbb{Q} , all two-component links which contain the square knot and from which $(S^1 \times S^2) \# (S^1 \times S^2)$ can be obtained by surgery. It was argued there that a certain family L_n of such links probably contradict the Generalized Property R Conjecture. Left unresolved was how the family L_n fits into the classification scheme. This question is resolved here, in part by giving varied perspectives and more detail on the construction of the L_n .

The Property 2R Conjecture [GST] (the simplest remaining case of the Generalized Property R Conjecture) proposes that any link of two components in S^3 , on which some surgery yields $(S^1 \times S^2) \# (S^1 \times S^2)$, can be changed to the unlink by a series of moves called handle-slides.

Let \mathcal{L} denote the set of all two-component links that contain the square knot Q and on which some surgery yields $(S^1 \times S^2) \# (S^1 \times S^2)$. It is argued in [GST] that there is an infinite family $L_n \subset \mathcal{L}$ of links that, for $n \geq 3$ probably do not satisfy the Property 2R Conjecture, for if one of the family did, then a corresponding presentation of the trivial group could be trivialized by Andrews-Curtis moves, an outcome that seems very unlikely. On the other hand, it is also shown that each link in the family can be handle-slid to the unlink, once a single canceling Hopf pair is added. Thus all of the L_n are consistent with a Weak Property 2R Conjecture, a conjecture that would suffice to prove the smooth 4-dimensional Poincaré Conjecture for homotopy spheres without 1-handles [GST, Proposition 9.2].

There is a straightforward classification of \mathcal{L} in [GST, Corollary 6.4], recounted here in Section 5: The classification assigns to each link a natural slope, indexed by those $\frac{p}{q} \in \mathbb{Q}$ for which q is odd. But the classification requires unspecified handle-slides of the other link component over Q and we were unable to resolve in [GST] how the family L_n fits into this classification. This left a puzzling gap ([GST, Question One]) between the 4-dimensional Kirby-calculus arguments (with 20-year-old

Date: August 8, 2012.

Research partially supported by National Science Foundation grants.

roots in [Go]) which gave rise to interest in L_n , and the 3-dimensional sutured manifold arguments which were used to classify \mathcal{L} . Here we resolve that question by showing that each L_n corresponds to the slope $\frac{n}{2n+1} \in \mathbb{Q}$. So the family L_n constitutes a relatively small subset of \mathcal{L} and, in particular, it remains possible (though unlikely) that some link in \mathcal{L} could still be a counterexample even to the Weak Property 2R Conjecture.

1. CONSTRUCTION OF THE L_n - A REVIEW

Here is a brief review of the relevant material from [GST, Figure 19]. Any closed orientable 3-manifold can be obtained from S^3 by surgery on a framed link [L]. The Kirby calculus [Ki1] provides two operations on framed links, each of which has no effect on the resulting 3-manifold; indeed, any two surgery descriptions of the same 3-manifold differ only by some sequence of these operations. One of the two moves is called a *handle slide* (reflecting its effect on the 4-manifold trace of the surgery). Such a handle-slide requires a choice of a band in S^3 connecting two components of the link. It has seemed a reasonable conjecture (motivated by the smooth 4-dimensional Poincaré Conjecture and called the Generalized Property R Conjecture) that any framed r -link description of the connected sum $\#_r(S^1 \times S^2)$ can be reduced to the 0-framed unlink of r components by some sequence of handle slides. The simplest unknown case $r = 2$ of the Generalized Property R Conjecture is called the Property 2R Conjecture.

A central point of [GST] is that a certain family $L_n, n \geq 3$ of 2-component links containing the square knot Q (shown in [GST, Figure 19]) is unlikely to satisfy Property 2R.

Let M denote the 3-manifold obtained from S^3 by 0-framed surgery on Q . The family $L_n = Q \cup V_n$ (called $L_{n,1}$ in [GST]) has these central features:

- L_0 can be handle-slid to be the unlink in S^3 . (This is demonstrated in [GST, Figures 12, 13, 5].)
- In M there is a simple closed curve α lying on a torus T so that each V_n intersects T twice and twisting V_n in M at T along the slope given by α converts V_n to V_{n+1} .
- When viewed in S^3 , the framing of α given by its annular neighborhood in T is ± 1 .

It is shown that, given these features, L_{n+1} can be obtained from L_n by handle-slides and the introduction and use of a single canceling Hopf pair. It follows inductively that, with the introduction of a canceling

Hopf pair, each L_n can be handle-slid to the unlink. In particular, 0-framed surgery on each L_n gives $(S^1 \times S^2) \# (S^1 \times S^2)$.

A second point of [GST], coming from sutured manifold theory, is that there is a natural classification (up to handle slides over Q) of all two-component links \mathcal{L} that contain the square knot Q and on which some surgery yields $(S^1 \times S^2) \# (S^1 \times S^2)$. In brief: for any link $Q \cup K \subset \mathcal{L}$, handle-slides of K over Q will eventually transform K to a curve that lies in the standard genus 2 Seifert surface F of Q , and furthermore its position in F is very constrained: viewing F as the 2-fold branched cover of a 4-punctured sphere P , K must be a homeomorphic lift of an embedded circle in P . There is a natural way of parameterizing embedded circles in P by the rationals; with one such parameterization, a circle in P lifts homeomorphically to F if and only if the corresponding rational has odd denominator.

A frustrating aspect of this classification is that each handle-slide of K over Q requires the choice of a band over which to slide, and the classification does not give a prescription for finding the relevant bands. So there is no way to see how any given link in \mathcal{L} fits into the classification. In particular, [GST, Question 1] asks, and here we answer, how the specific family of links L_n fits into this classification scheme. The argument is largely pictorial and includes also more detail on some of the transition between figures in [GST]. It is likely to be indecipherable without viewing a full-color rendering (e. g. the .pdf file).

2. FROM SURGERY DIAGRAM TO EXPLICIT LINK

We begin by explaining with pictures the transition in [GST] from a fairly simple surgery diagram of a probable counterexample to Property 2R to an explicit picture of it as a complicated link in S^3 . Begin with the surgery diagram Figure [GST, Figure 12d] and draw it symmetrically, a transition illustrated in Figure 1.

Next consider the effect of blowing down the red circles in the surgery description labelled $[\pm 1]$. Focus on the right circle and recall the easy fact (see [GS, Figure 5.18]) that blowing down the circle with label $[-1]$ is equivalent to taking the disk D that it bounds and giving everything that runs through it a $+1$ (sic) twist. In this case, part of what runs through D are n segments of a 0-framed component coming from the $+n$ twist-box on the right. Figure 2 is meant to illustrate what happens, very specifically in the top row for $n = 2$. Before twisting along D , move the $n = 2$ punctures in D so that as one moves clockwise around the disk, the punctures become more central. The track of the 2 strands

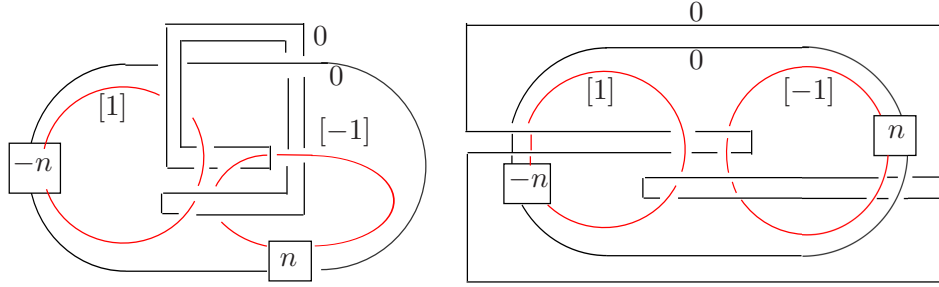


FIGURE 1.

going through D , after the $+1$ twist around D , is shown in red. It is then illustrated in blue how the result can be thought of as a $+1$ twist box placed around an n -stranded band that follows the original red circle that was blown down. The result for general n is shown next, and then this is applied to the given surgery diagram to give the link illustrated at the bottom of Figure 2. The gray annuli are meant to represent n parallel strands, much like the wide annuli that appear in [GST, Figure 1]. We now discuss the transition to that figure.

In Figure 3, the gray annuli are pushed off the plane of the green knot (now visibly the square knot), then the twist boxes are moved clockwise past one end of the two (black) connecting arcs, switching a crossing between the arc and the annulus to which it is connected. Finally, the two gray annuli are isotoped to push the parts containing the twist boxes to the outside of the figure, beginning to imitate their positioning in [GST, Figure 1].

Continue with the positioning, moving clockwise from the upper left in Figure 4. The first step there is to move the square knot into the correct position and then expand the two gray annuli. Next the ends of the connecting arcs on each annuli are moved to be adjacent (represented by the small blue squares in the figure). This has the psychological advantage that the link component V_n can be thought of as starting with a single circle (the end-point union of the two black arcs in the figure) and then doing a $\pm n$ Dehn twist to that circle along the cores of the two gray annuli. The next move is a surprise: push the blue square in the right hand gray annulus clockwise roughly three-quarters around the annulus, pushing the twist-box ahead of it. When this is done (the bottom left hand rendering) the picture of the link has become essentially identical to that in [GST, Figure 1].

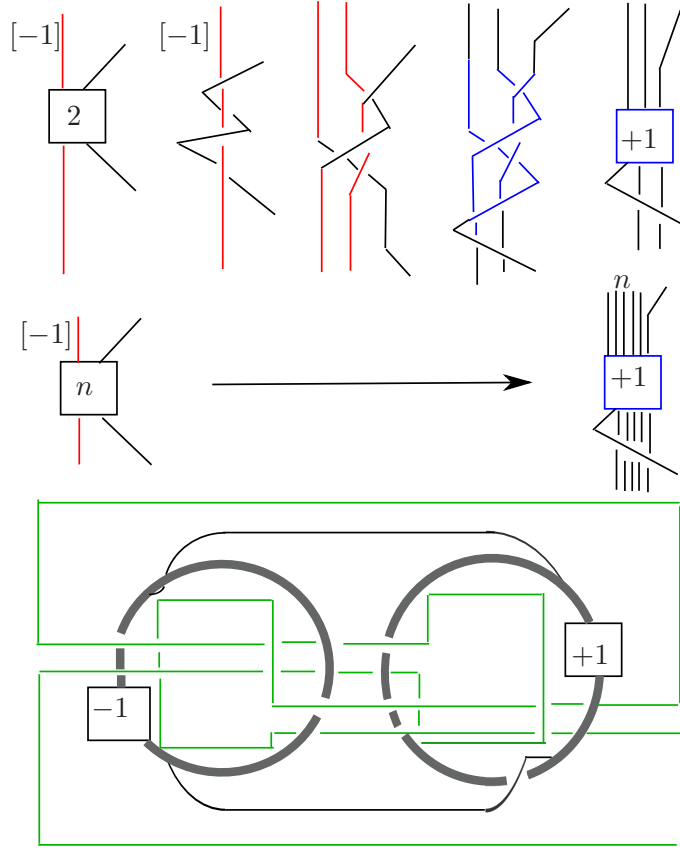


FIGURE 2.

3. PUSHING V_n ONTO A SEIFERT SURFACE

It follows easily from [ST, Corollary 4.2] that each V_n , perhaps after some handle-slides over Q , can be placed onto a standard Seifert surface of Q , so that the framing of V_n given by the Seifert surface coincides with 0-framing in S^3 . (For details, see the proof of [GST, Theorem 3.3].) The proof of [ST, Corollary 4.2] requires Gabai's deep theory of sutured manifolds. It is non-constructive and in particular the proof provides no description of how to find the handle-slides of V_n over Q that are needed to place V_n onto the Seifert surface.

In this section we begin the search for the required handle-slides by trying to push the whole apparatus A that defines V_n onto a Seifert surface F for Q . (Here A is the union of the two gray annuli in Figure 2 with the two arcs that connect them.) It's immediately clear that A can't be completely moved onto F , since each of the gray annuli in A

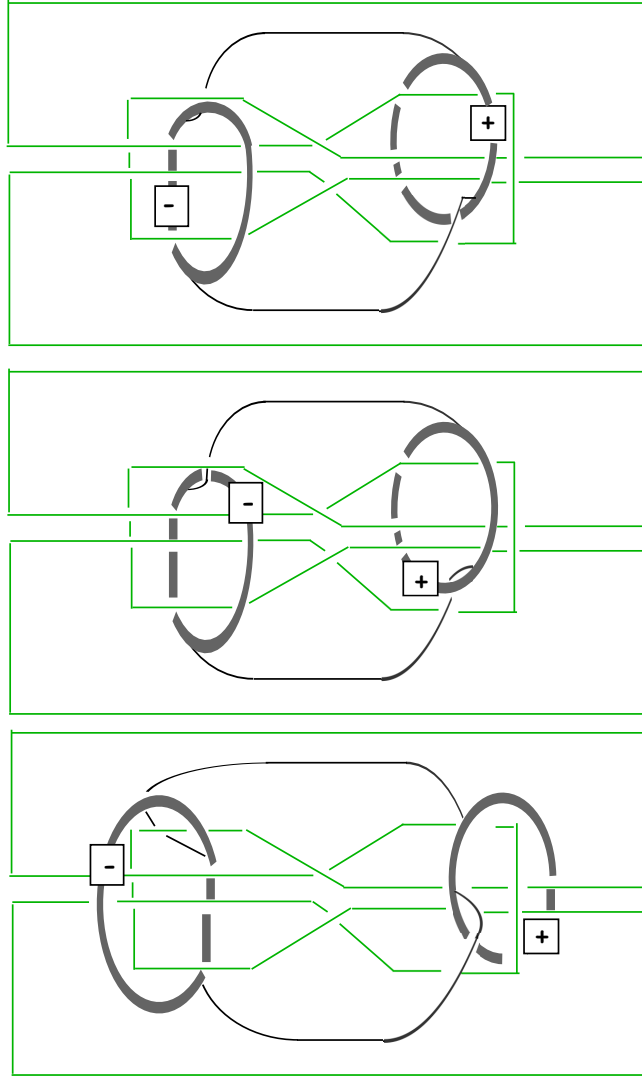


FIGURE 3.

has non-trivial linking number with Q . Here we focus on getting A as closely aligned with F as seems possible, given this difficulty.

Figure 5 repeats the first two steps in Figure 3, with these minor modifications:

- The square knot Q is laid out in the classic fashion that emphasizes its Seifert surface: three rectangles in the plane of the page, with the middle rectangle joined to each of the side rectangles via three twisted bands.

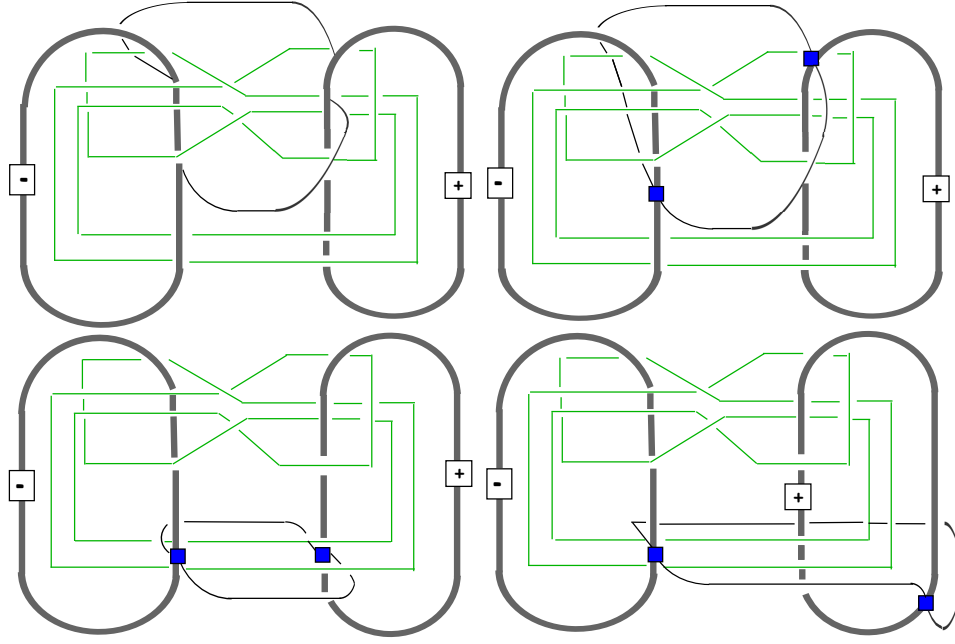


FIGURE 4.

- The Seifert surface F is not shown; instead, the annuli have been shaded to show where they lie in front of or behind F .
- In the lower figure, not only has each twist box been passed through an end of one of the arcs (as was done in Figure 3), but also the annuli have been stretched horizontally and the top subarc of the top annulus passed over the top subarc of Q (and symmetrically at the bottom) so that much of each annulus lies right next to F .
- Since each gray annulus links Q once, there is an intersection point (shown with a red dot in the lower figure) of each with F .
- The arcs connecting the annuli appear in red.

Further progress is shown in Figure 6: first the red arcs are moved mostly onto F by passing one of them over the top (and the other under the bottom) of the center of Q . (In fact, if the red arcs were not attached to the annuli at the blue squares, but set free to form their own circle, that circle could be moved entirely onto F away from the annuli.) Then the subarcs of the annuli at the center of the figure are moved to conform to F as much as possible, at one point inevitably passing from the top of F , around Q and then under F . Each annulus conforms even more closely to F if half of its full twist is absorbed into the point at which the annulus is passed around Q , moving from the

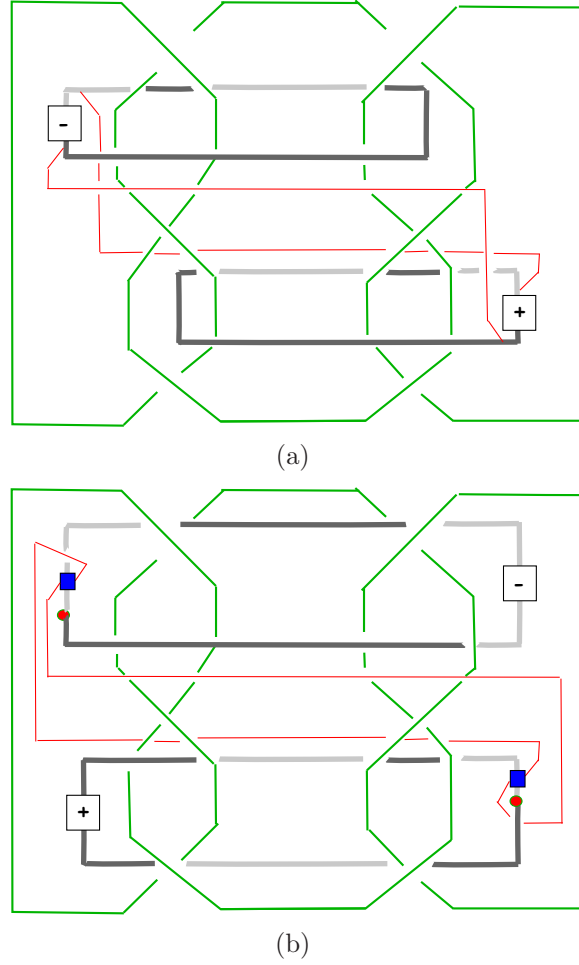
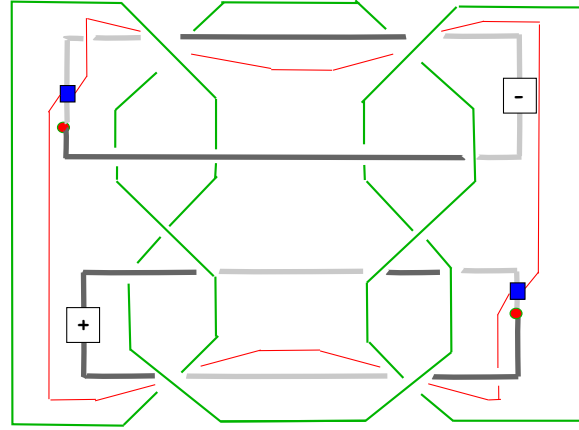


FIGURE 5.

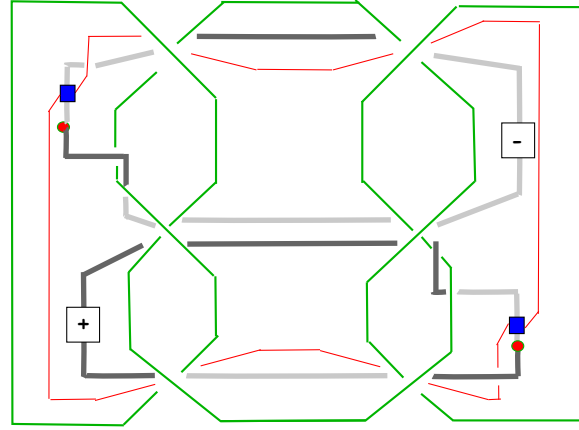
top of F to the bottom. The final result is shown in Figure 7. Further hope of pushing each V_n onto F requires a good understanding of the fiber structure of the complement of Q and the parallel fiber structure of the closed 3-manifold M obtained by 0-framed surgery on Q . That is the subject of the next section.

4. THE FIBER STRUCTURES OF $S^3 - Q$ AND M

For understanding the structure of the fibering of $S^3 - Q$, a good starting point is the fibering of the trefoil knot. (In discussing knot complements, we'll suppress the distinction between a knot and its regular neighborhood in S^3 . Thus $S^3 - Q$ will be shorthand for the compact manifold with torus boundary that is the complement in S^3



(a)



(b)

FIGURE 6.

of an open regular neighborhood of Q .) A nice account of this fibering is given in [Z, Section 3] beginning with Zeeman's modest: "I personally found it hard to visualise how the complement of a knot could be fibered so beautifully, until I heard a talk by John Stallings on Neuwirth knots." The classic description is to view the punctured torus Seifert surface S_+ of the trefoil knot Tr_+ as two disks connected by three twisted bands. The monodromy of Tr_+ cycles the three bands and exchanges the two disks, and so ends up being of order six. At each iteration of the monodromy the knot itself is rotated a sixth of the way around. A dual view of the monodromy will be more useful here: pick one vertex in the center of each of the two disks in S_+ and connect these two vertices by three edges, each running through one of the

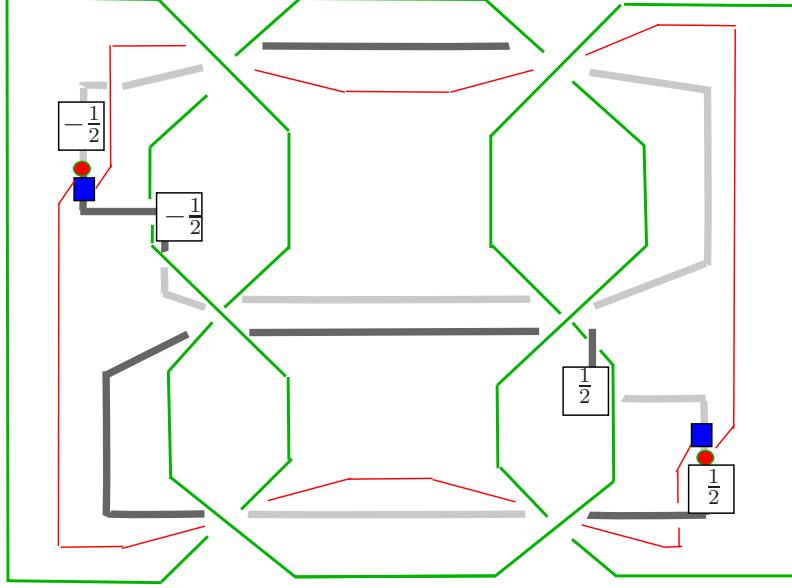


FIGURE 7.

twisted bands in S_+ . If S_+ is cut open along this θ graph, the result can be viewed as a planar hexagon with a disk removed. The circle boundary of the removed disk corresponds to Tr_+ , and S_+ itself can be recovered by identifying opposite sides of the hexagon, as in Figure 8(a). The period six monodromy is then just a $\frac{\pi}{3}$ rotation of the punctured hexagon and we can view $S^3 - Tr_+$ as the mapping torus of S_+ under this monodromy. If we were interested in the closed manifold obtained by 0-framed surgery on Tr_+ , the picture would be the same, but with the disk filled in.

The square knot Q is the connected sum of two trefoil knots Tr_{\pm} , one right-handed and the other left-handed. One way to see the monodromy of the Seifert surface S_- of the other trefoil Tr_- is to use Figure 8(a), but, in order to obtain the opposite orientation, first reflect the figure across the inner (circle) boundary component, so the hexagonal boundary lies on the inside and the knot boundary Tr_- on the outside, as in Figure 8(b). The complement of Tr_- is then the mapping torus of S_- under the monodromy shown in Figure 8(b).

Since Q is the connected sum of Tr_{\pm} it is easy to see that $S^3 - Q$ can be obtained by gluing the manifolds $S^3 - Tr_+$ and $S^3 - Tr_-$ along a meridional annulus in the boundary of each. A meridional annulus in the mapping torus picture of the knot complements is the mapping torus of a subinterval of ∂S_{\pm} , so the result of gluing together the two knot complements along a meridional annulus of each is the mapping

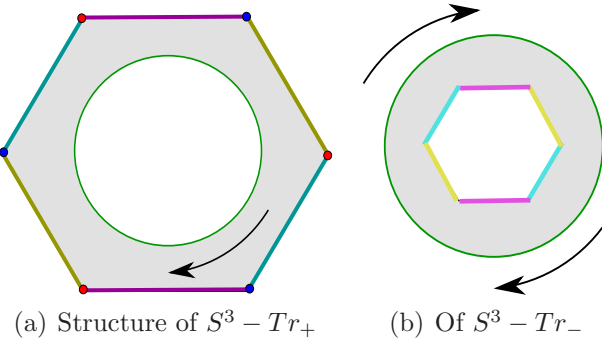


FIGURE 8.

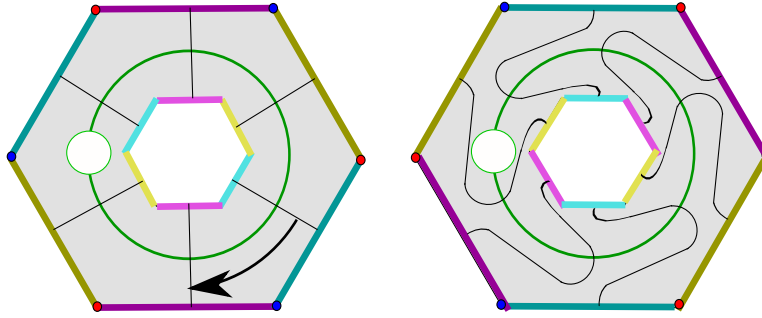


FIGURE 9.

torus of the monodromy shown in Figure 9. Note that the monodromy is a bit more complicated than it first appears (on the left): in order to make the monodromy preserve the boundary circle (corresponding to the knot Q) the $\frac{\pi}{3}$ rotation must be undone near the central circle, as shown on the right of Figure 9. This complication disappears in a description of the manifold M however, because the boundary circle is filled in with a disk, so M is simply the mapping cylinder of the $\frac{\pi}{3}$ rotation of F_{\cup} shown in Figure 10.

To understand how the monodromy acts on $F \subset S^3$ consider how the monodromy of the trefoil knot acts on, say, the left half F_{ℓ} of Figure 6(b) and double this to get the action on all of F . This process is described in three steps in Figure 11. On the left are shown how the three arcs corresponding to the pairwise identified sides of the hexagon in Figure 8(a) appear in F_{ℓ} . The arcs connect the red vertex to the blue vertex and are oriented so that the monodromy takes the top arc to the middle arc and the middle arc to the bottom arc. The monodromy also takes the bottom arc to the top arc, but reverses the orientation, reflecting the fact that the monodromy is of order six. Red, blue and

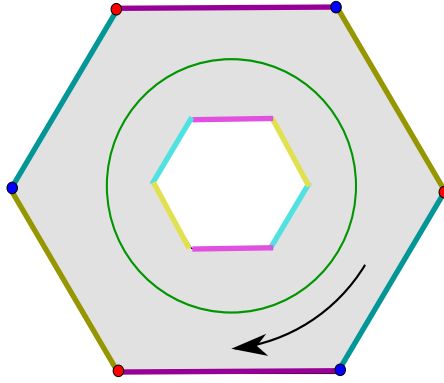
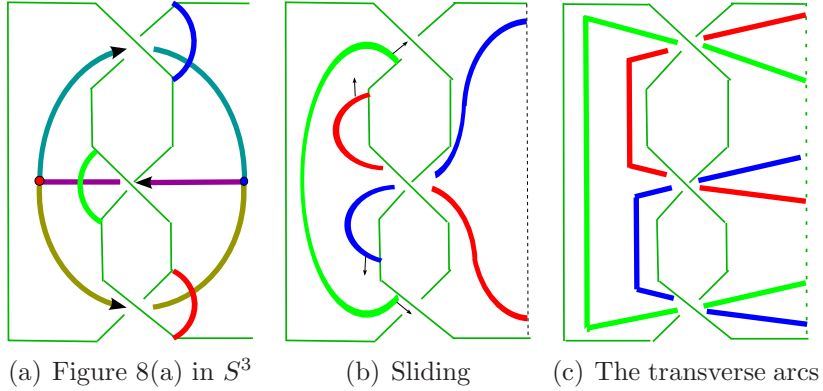
FIGURE 10. Structure of M 

FIGURE 11.

green properly embedded transverse arcs in F_ℓ are added to the figure, and in Figure 11(b) these are slid along the trefoil knot until their ends lie on the vertical arc along which F_ℓ is doubled to recover F (Figure 11(c)). When the red, blue and green arcs are doubled they become three circles in F which are permuted by the monodromy on F_\cup . Figure 12 shows the three circles as they appear in $F \subset F_\cup$, the fiber of M , and how they appear in F , the Seifert surface of Q in S^3 .

Note that the three circles in F bear a striking resemblance to the two gray annuli and the red circle of Figure 6(b). We can exploit the resemblance to give a color-coded description of how the apparatus A defining V_n can be viewed in the hexagonal model of the monodromy of F_\cup . Picture $S^3 - Q$ as the hexagonal picture of $F \times I$ with the top $F \times \{1\}$ identified to the bottom $F \times \{0\}$ by the monodromy twist. Imagine how A would look, viewed from above (i. e. looking down at the top $F \times \{1\}$) after coloring the upper gray annulus in Figure 7 red,

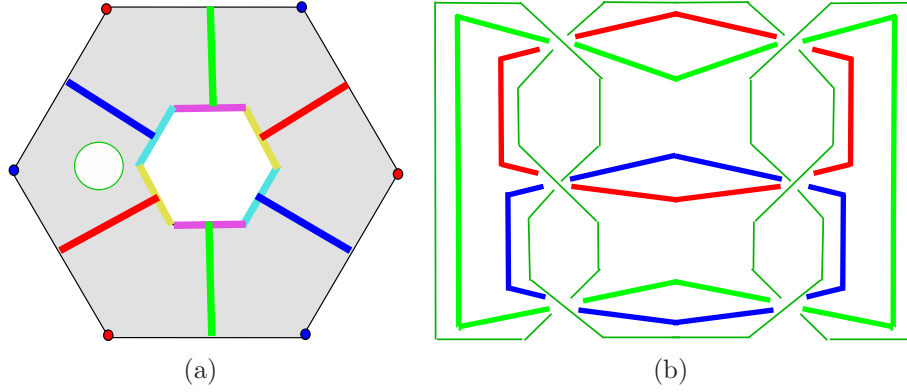


FIGURE 12.

the lower gray annulus blue, and the connecting arcs yellow. This is shown in Figure 13: away from $\partial F \times I$ the annuli lie near $F \times \{\frac{1}{2}\}$. As the left ends of both the red and blue annuli are incident to $\partial F \times \{\frac{1}{2}\}$ they rise along $\partial F \times I$ until they pass out of the top $F \times \{1\}$ (represented by a green dot) and continue their rise from the bottom $F \times \{0\}$ until they reach $\partial F \times \{\frac{1}{2}\}$ again and are joined to the rest of the red and blue annuli there. The switch in perspectives (the annuli climbing the vertical wall $\partial F \times I$ rather than circling around the knot Q) changes the apparent sign of the half-twist at $\partial F \times \{\frac{1}{2}\}$ from $\pm\frac{1}{2}$ in Figure 7 to $\mp\frac{1}{2}$ in Figure 13, much as the apparent half-twist on a ribbon in a book cover will change sign when the book is fully opened (see Figure 14). The upshot is that the apparent framing of both the blue and red annuli in Figure 13 is now zero, the “blackboard framing”.

Begin a process of pushing V_n in M until all of V_n lies at the level $F_\cup \times \{\frac{1}{2}\}$. First compare Figures 13 and 15: Since the isotopy will be in M , $F \times I$ has been replaced by $F_\cup \times I$, filling in the missing disk, with only the two green dots remaining. The green dots continue to represent the points at which the piece of the red and blue annuli to the right of the dots emerge from the top of the box $F_\cup \times I$ and, simultaneously, where the red and blue annuli to the left of the dots enter the bottom of $F_\cup \times I$. (A vertical cross-section of the northwest sextant, roughly parallel to the blue annulus, appears in Figure 17.) One of the two arcs in A that connects the red annulus to the blue annulus has changed color from yellow to brown. This will be the arc β that is pushed first through the top of the box. The point at which β is incident to the blue annulus has been slid in $F_\cup \times \{\frac{1}{2}\}$ so that it lies just to the left of the green dot instead of to the right. Now push β through the top of the box, at which point it reappears in M

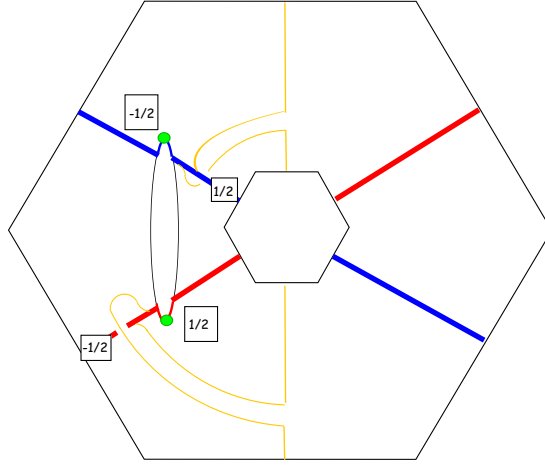


FIGURE 13.

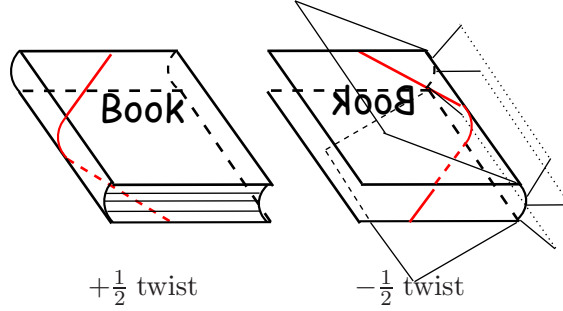


FIGURE 14.

at the bottom of the box, but, because of the monodromy, with a $\frac{\pi}{3}$ clockwise rotation of the ends of β on the inner and outer hexagons. The result, after also sliding the end of β on the red annulus back to its original position to the left of the green dot, is shown in Figure 16. The movement of the end of β at the blue annulus is shown schematically, clockwise from the upper left, in Figure 17.

A symmetric argument describes how to push *down* the other arc (shown in yellow) that connects the blue and red annuli. The result is shown in two steps in Figures 18(a) and 18(b). The more pleasing Figure 18(c) is then obtained by sliding the points where the arcs are incident to the annuli, so that they all appear on the right side of the figure. The red and blue annuli are now only $n - 2$ arcs wide, so in the case $n = 2$, Figure 18(c), with the red and blue annuli omitted, represents the final positioning of V_2 , completely on the surface F_\cup as was predicted to be possible.

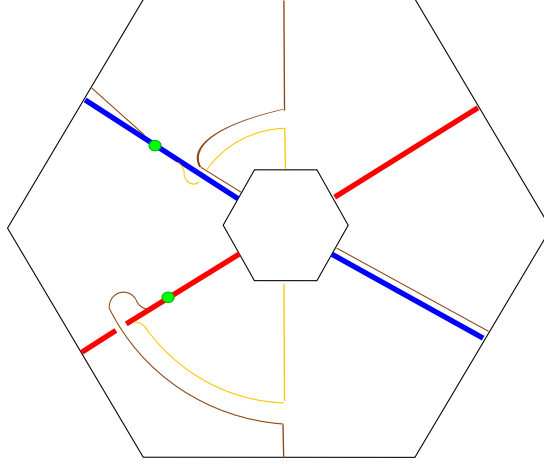


FIGURE 15.

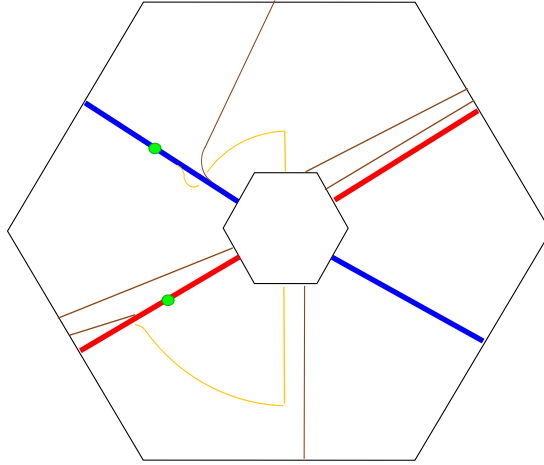


FIGURE 16.

If $n \geq 3$ further moves of V_n are required. Figures 19(a) and 19(b) show two more upward pushes of the brown arc β through the top of the box $F_\cup \times I$ and, via the clockwise $\frac{\pi}{3}$ rotation of the monodromy, back through the bottom of the box. (Figures 20(a) and 20(b) show the corresponding final position of $V_n, n = 3, 4$ on a fiber F_\cup of M .) The fact that, after the push, a segment of β crosses *over* over the blue annulus (and another crosses over the red annulus) is at first puzzling. But recall how the monodromy acts on F_\cup : Up to isotopy, it is a $\frac{\pi}{3}$ clockwise twist, but it also fixes the green dots in the figure (the points where the blue and red annuli intersect the top and the bottom of the box $F_\cup \times I$). So the monodromy itself looks a bit like that in Figure 9.

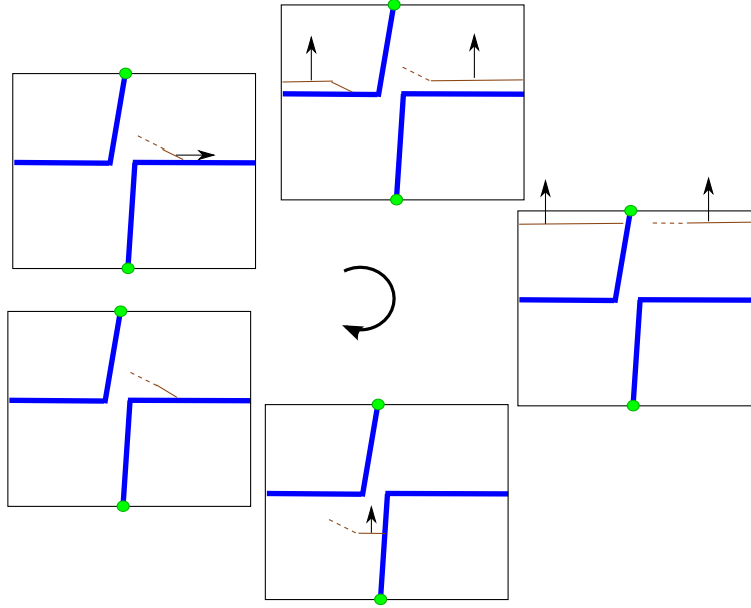


FIGURE 17.

Thus a segment of β spanning the southern sextant of F , when pushed out the top of $F \times I$ and reappearing at the bottom, has its ends rotated to the southwest sextant, but the middle of the segment will pass south of the green dot on the red annulus. The segment does then pass under the red annulus, but the segment can be straightened by an isotopy that appears to move the segment from below the annulus to above the annulus. See Figure 21, which also shows the isotopy in a vertical cross-section near the red annulus in the southwest sextant. Similar remarks apply to segments of β passing over the blue annulus.

The final appearance of V_n on the fiber of M depends mostly on $n \bmod 3$. Figure 22 shows the general case for $n \equiv -1, 0, 1$ by depicting with brown bands collections of $j - 1$ parallel segments of β . The blue and red annuli in the figures can be ignored; they have been included only to help imagine the transition from one step to the next. At several places in the figure it appears that a single segment of β intersects a brown band, but this is just shorthand for a double-curve sum of the crossing arc with the $j - 1$ curves in the band, as shown in Figure 22(a).)

Of course all these presentations of $V_n \subset F_\cup \subset M$ can be translated to pictures of $V_n \subset F \subset S^3$. This translation, in the case $n = 3$, is shown in Figure 23 via a three-stage process: The points in which V_n intersects the circle separating the trefoil summands are labeled

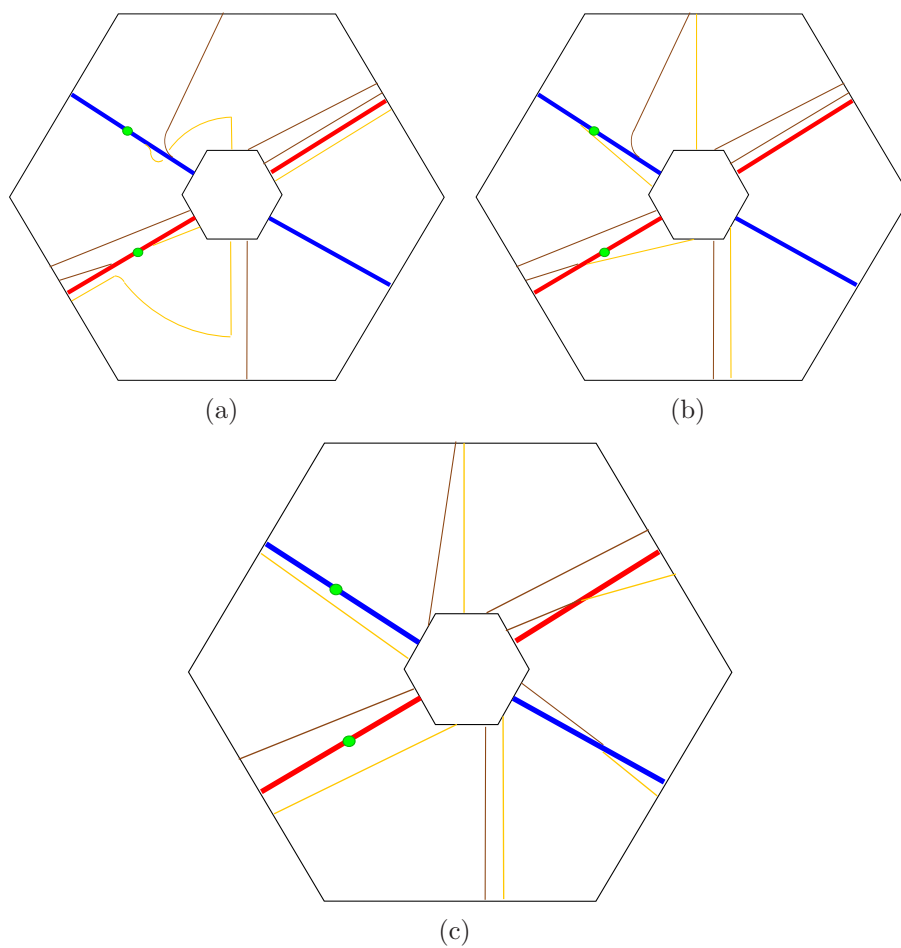


FIGURE 18.

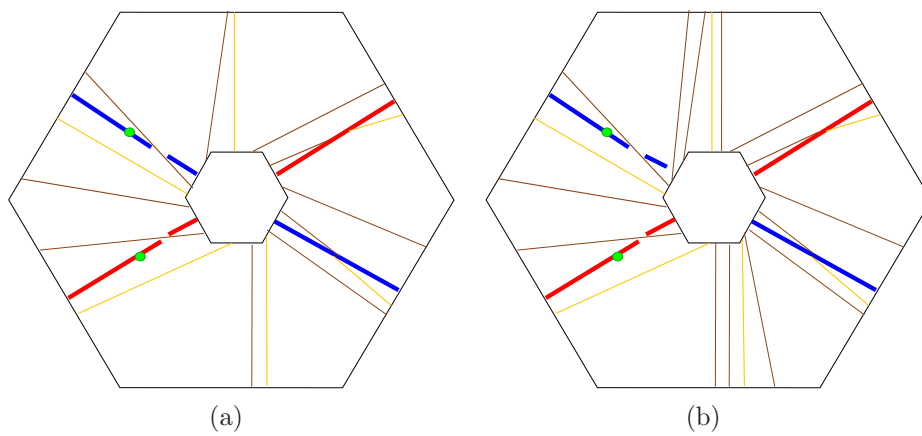


FIGURE 19.

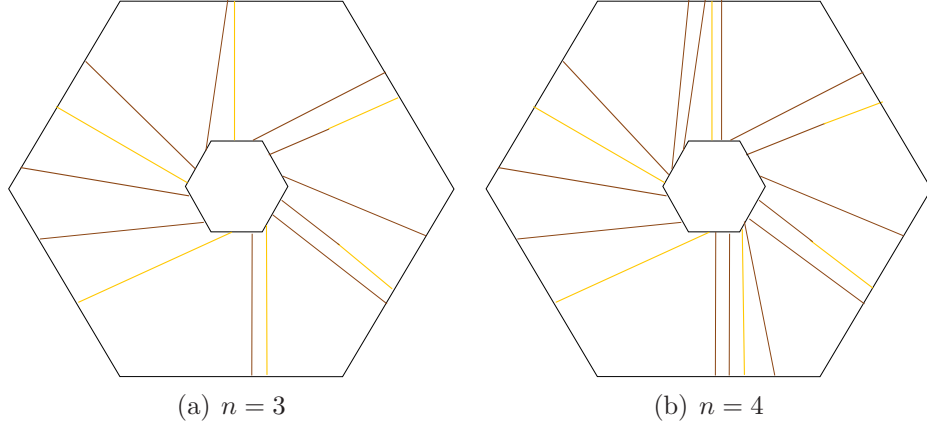


FIGURE 20.

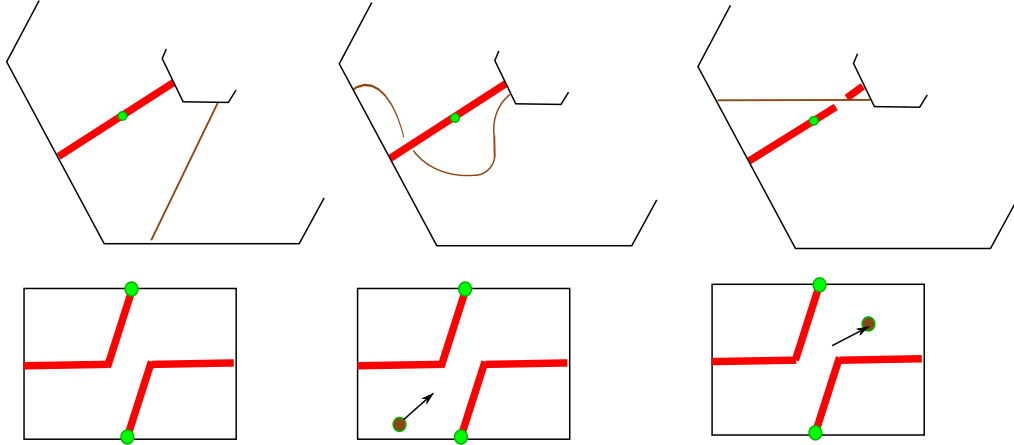


FIGURE 21.

sequentially, as shown in Figure 23(a). Then the discussion around Figure 11 is used to locate each of these subarcs in the appropriate place on the Seifert surface $F \subset S^3$, as shown in Figure 23(b). These subarcs are mostly joined along the arc that separates the left- and right-hand trefoil knots, but there is a dangling end at both the top and the bottom of F in the figure, reflecting that joining these ends by a subarc requires a choice of how V_n is to avoid the disk $F_\cup - F$ bounded by Q . The choice is whether to connect these ends by an arc parallel to the trefoil knot on the left or parallel to the one on the right. Figure 23(c) shows the result when the two ends are connected along the trefoil on the left, via an arc that is rendered in red. The resulting link in S^3 is slice by construction; it is a nice question (just as it was

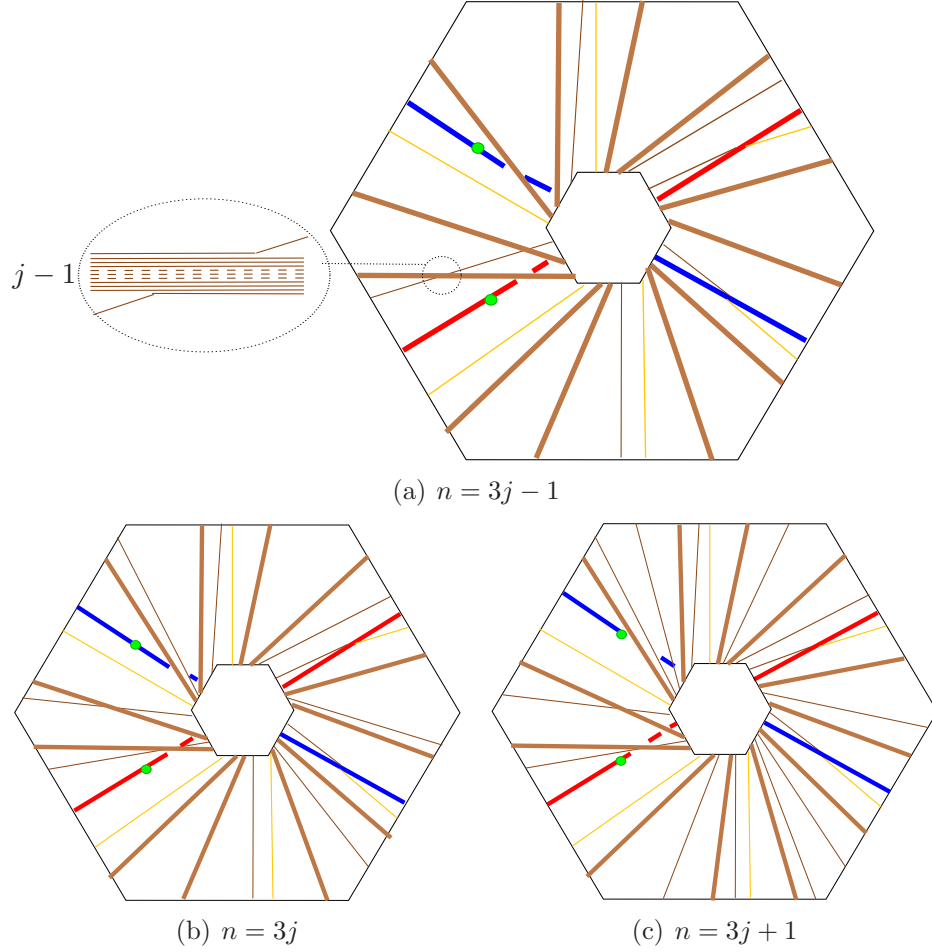
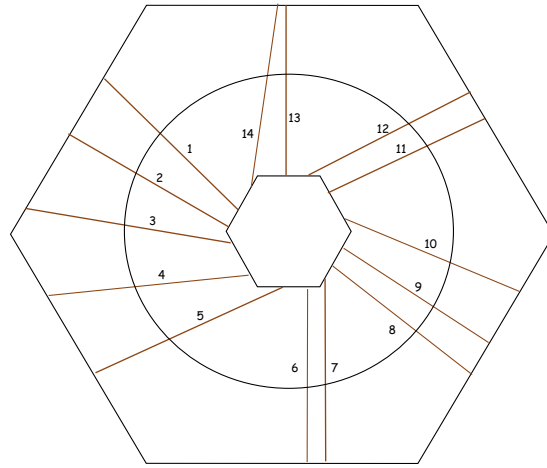


FIGURE 22.

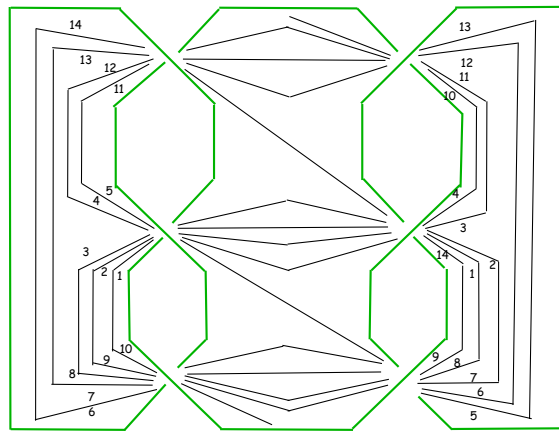
for [GST, Figure 2]) whether this link, or examples from higher n , are also ribbon links.

5. THE CURVE THAT V_n COVERS IN A 4-PUNCTURED SPHERE

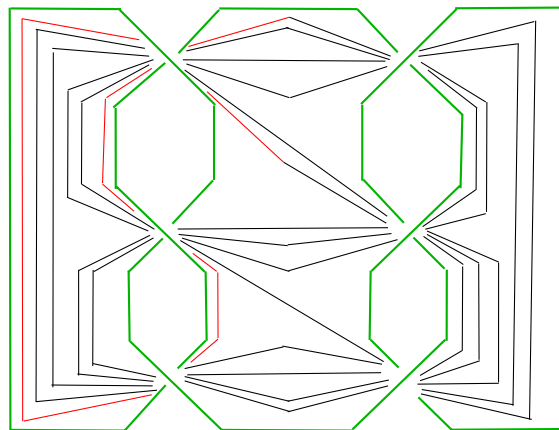
Recall from [GST] that there is a natural \mathbb{Z}_3 action on the genus 2 surface F_\cup , by which F_\cup is a 3-fold branched cover of S^2 with 4 branch points. See [GST, Figure 7], reproduced as Figure 24 here. It is further shown ([GST, Corollaries 6.2, 6.4]) that 0-framed surgery on a simple closed curve $V \subset F_\cup \subset M$ yields $(S^2 \times S^2) \# (S^2 \times S^2)$ if and only if V projects homeomorphically to an essential simple closed curve in the 4-punctured sphere $P = S^2 - \{\text{branch points}\}$ and that an essential simple closed curves in P is the homeomorphic image of a curve in F_\cup if



(a)



(b)



(c) Is it a ribbon link?

FIGURE 23.

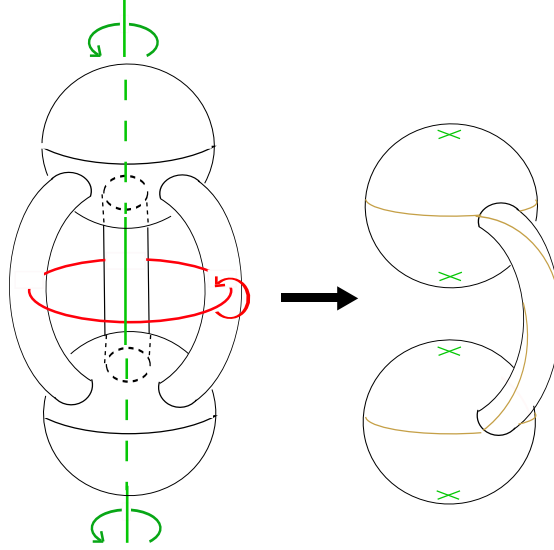


FIGURE 24.

and only if it separates two branch points coming from the same trefoil summand of Q .

The hexagonal description of F_\cup given in Section 4 (e.g. Figure 10) is particularly easy to see as a branched cover over S^2 . Start by giving S^2 the “pillowcase” metric: view S^2 as constructed from two congruent rectangles, with their boundaries identified in the obvious way. The corners of the rectangles will be the branch points for the covering and the two rectangles will be called the front face and the back face of $P \subset S^2$. Identify the top sextant of Figure 10 with the front face of P and wrap the other five sextants equatorially around P . See Figure 25. Then the northeast, northwest and the bottom sextant are all identified with the back face of P and the southeast and southwest sextants with the front face. The identifications of the boundary edges in Figure 10 are consistent: for example the top and bottom edges of the outside hexagon in the figure have been identified with the top edge of, respectively, the front and the back face of P , so the identification of these edges to create F_\cup is consistent with the identification of the top edges of the two rectangles to form S^2 .

There is a natural correspondence between isotopy classes of simple closed curves in P and the extended rationals $\mathbb{Q} \cup \infty$. The correspondence is given by the slope in the pillowcase metric. It is a bit more useful in our context to take the reciprocal of the apparent slope in Figure 25 or, equivalently, to turn the pillowcase in the figure on its side. Thus one of the horizontal curves in P shown in Figure 25 has

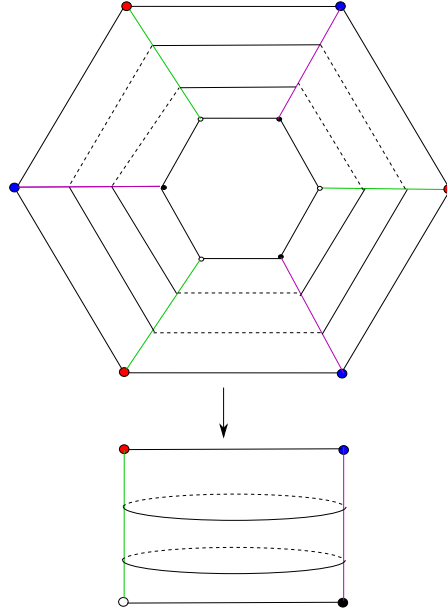


FIGURE 25.

slope 0, so it will correspond here to $\frac{1}{0} = \infty \in \mathbb{Q} \cup \infty$. Such a curve is 3-fold covered by a simple closed curve in F_\cup that divides F_\cup into the two genus-one surfaces F_ℓ and F_r , Seifert surfaces for the two trefoil summands of Q . A simple closed curve in P separates the two branch points lying in F_ℓ (equivalently, separates the two that lie in F_r) if and only if it intersects the top seam of the pillowcase in an odd number of points; that is, if and only if it corresponds to a fraction $\frac{p}{q} \in \mathbb{Q} \cup \infty$ for which q is odd. So, for example, a circle in P that is vertical in Figure 25 is assigned $0 = \frac{0}{1} \in \mathbb{Q}$ and corresponds to any of the three unknotted circles in F shown in Figure 12(b). In this manner, $\{p/q \in \mathbb{Q} \mid q \text{ odd}\}$ becomes a natural index for the set of curves $V \subset S^3 - Q$ such that surgery on $Q \cup V$ gives $(S^1 \times S^2) \# (S^1 \times S^2)$. (Since $\infty = \frac{1}{0}$ does not have odd denominator, we can ignore it.) It is natural to ask exactly how the curves V_n fit into this classification scheme.

Remark: Here is the rationale for taking the reciprocal of the apparent slope, i. e. for turning Figure 25 on its side. There is a natural automorphism $(S^3, Q) \rightarrow (S^3, Q)$ called a *twist* (see [Z] for a related use of the term). A twist fixes one of the trefoil summands of Q and rotates the other trefoil summand fully around the two points at which the summands are joined. (A more technical description: a twist is a meridional Dehn twist along a follow-swallow companion torus for Q .)

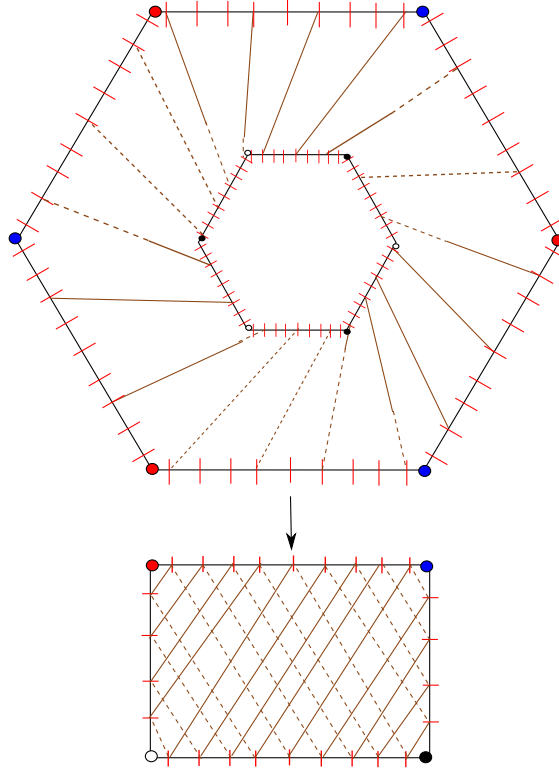


FIGURE 26.

It's fairly easy to see that a twist changes a curve $V \subset F$ indexed by $\frac{p}{q} \in \mathbb{Q} \cup \infty$ to one indexed by $\frac{p \pm q}{q} \in \mathbb{Q} \cup \infty$. So if we also allow V to change by such twists of Q , which do not change the isotopy class of the link $Q \cup V$, as well as by isotopy and slides of V over Q , we could even index the curves V by $\frac{p}{q} \in \mathbb{Q}/\mathbb{Z}$, q odd and, as a result, focus attention on those indices $\frac{p}{q}$ in which $|2p| < q$.

Theorem 5.1. *In the classification scheme above, the curve V_n corresponds to $\frac{n}{2n+1} \in \mathbb{Q}$.*

Proof. Examine Figure 22, ignoring the red and blue bands and recalling that each wide brown arc represents $j-1$ parallel arcs. The number of intersection points of V_n with the outer hexagon is the total number of arcs that appear, $4n+2$. The number of intersection points of V_n with the six lines that divide the figure into sextants is $2n$. The ratio is then $\frac{n}{2n+1}$. \square

The case $n = 4$ is shown in Figure 26.

GSTFig19.{ps,eps} not found (or no BBox)

FIGURE 27.

6. AN ALTERNATE VIEW OF THE CONSTRUCTION

Essentially the first step in the construction above (see Figure 2) was to import [GST, Figure 12] and blow down the two ± 1 bracketed unknots. There is another way to organize the construction, one which delays the blow-down until much later and so gives additional insight into how V_n lies in M . Begin with the link diagram [GST, Figure 19] (a version of [GST, Figure 11]) that describes L_n . This is shown here in Figure 27, augmented so that the relevant torus $T \subset M$ is more visible: The vertical plane, mostly purple but containing a green disk, is a 2-sphere in S^3 that contains a circle on which 0-framed surgery is performed. The surgery splits the 2-sphere into a pair of 2-spheres, one green and one purple. In the diagram the two 2-spheres are connected by two thick pink strands. The torus T is obtained by tubing the two 2-spheres together along the annuli boundaries of the two pink strands. The $\pm n$ twist-boxes represent the n -fold Dehn twist along the meridian of T used in the construction of V_n (see [GST, Section 10]).

Figure 28 shows a sequence of isotopies which moves the link in Figure 27 (including the bracketed unknots) to a position in which something like the square knot begins to appear. When the top black circle is slid over the two red circles labeled $[\pm 1]$ the square knot fully emerges: Figure 29 shows the resulting circle as a green square knot, on which 0-surgery is still to be performed, and also illustrates how the bracketed red circles can be pushed near its Seifert surface. (The dotted parallel green and red arcs in the twist boxes are to indicate that the twisting is of the black curve around the red and green curves, not the red and green curves around each other.)

In fact it is shown in Figure 30 that, except for the twist boxes, both the red curves (labeled $[\pm 1]$) and the 0-framed black curve can be simultaneously pushed onto the natural Seifert surface of the green square knot, all before the bracketed red curves are blown down! (The apparent twist of the curves in Figure 30(a) is canceled by a symmetric twist of the curves on the left side of the twist boxes.)

When the square knot is straightened out, it appears as in Figure 31, which bears a striking resemblance to the earlier Figure 12(b). In particular, if we temporarily ignore the 0-surgered black curve (so we can also ignore the twist boxes), then the two red circles are parallel to each other in the *complement* of the square knot. That is, there is an annulus $A \subset S^3 - Q$ whose boundary consists of the two red

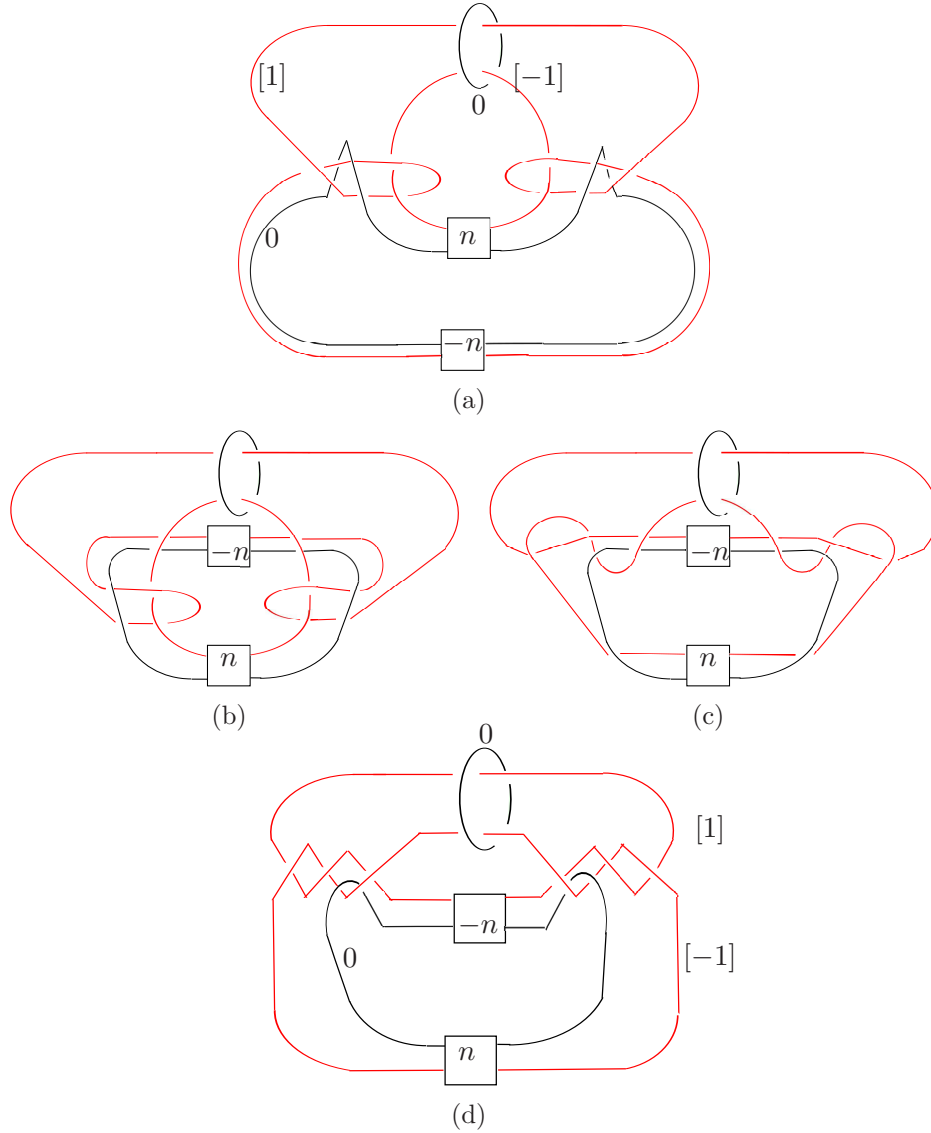


FIGURE 28.

circles. This can be seen directly in Figure 31, but it also follows from the discussion surrounding Figure 12(b): one red circle is the image under the monodromy of the other. Since the red circles have opposite (bracketed) signs, it follows that blowing both of them down simultaneously has no effect on the square knot: it persists after the blow-down, but any arc that intersects the annulus A between the red curves will be twisted around the core of A . In particular, the 0-surgered black curve intersects A n times at each of the upper and

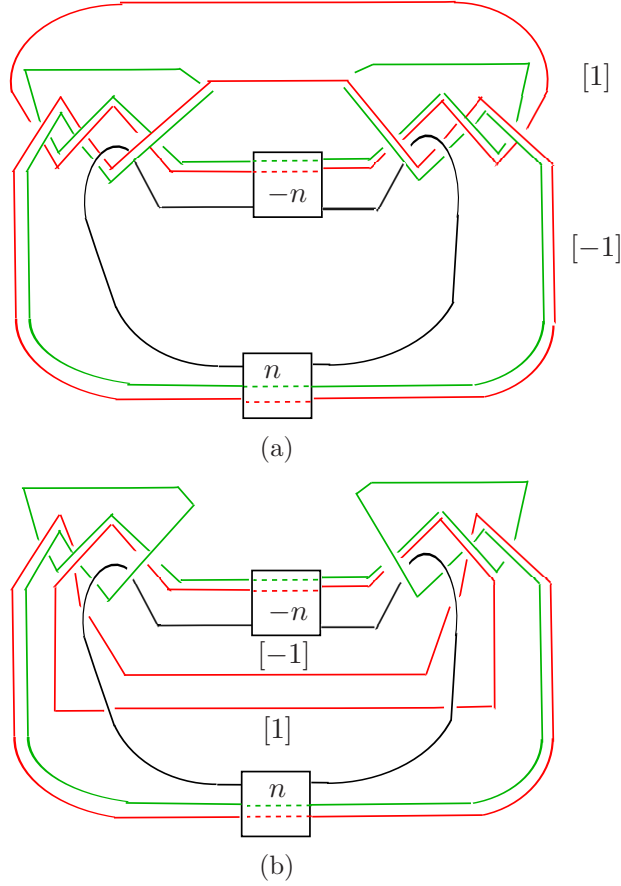
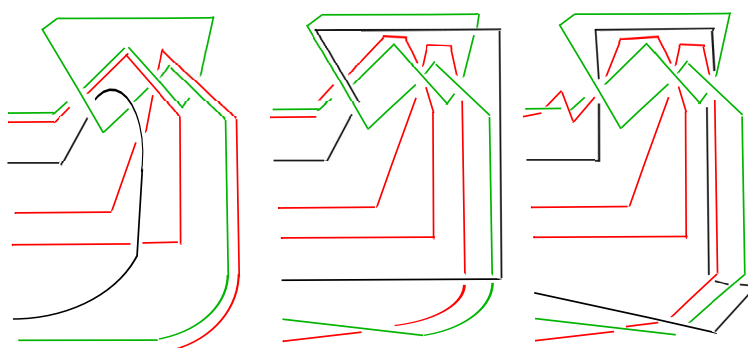


FIGURE 29.

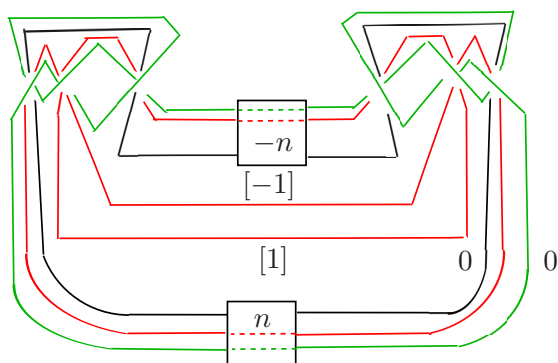
lower twist boxes, so the simultaneous blowdowns change Figure 31 to Figure 32 via a process akin to that shown in Figure 2. Finally, Figure 32 can be isotoped to Figure 6(b), at which point we rejoin the previous argument.

7. IDENTIFYING THE TORUS $T \subset M$

It is unsatisfying that in both views of the construction above it is hard to identify the torus $T \subset M$, whose critical properties are listed at the beginning of Section 1. T appears in [GST, Figure 19] (here in Figure 27), but the appearance is well before the bracketed red curves are blown down, and it is hard to track T through that operation. The most obvious torus in M is the swallow-follow torus in $S^3 - Q$, which is also the mapping torus of the green circle in Figure 10. This torus does indeed intersect V_0 in two points, but a little experimentation shows



(a)



(b)

FIGURE 30.

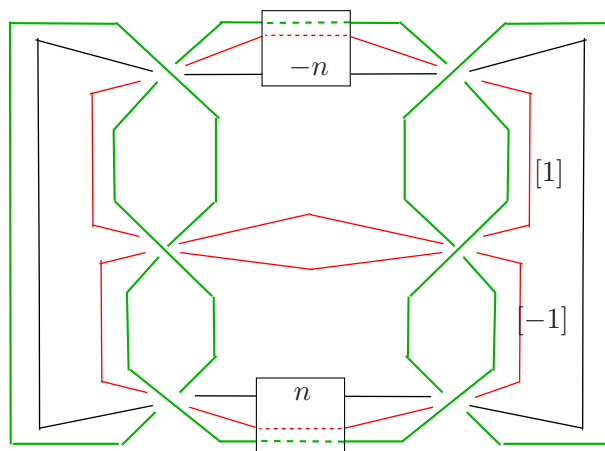


FIGURE 31.

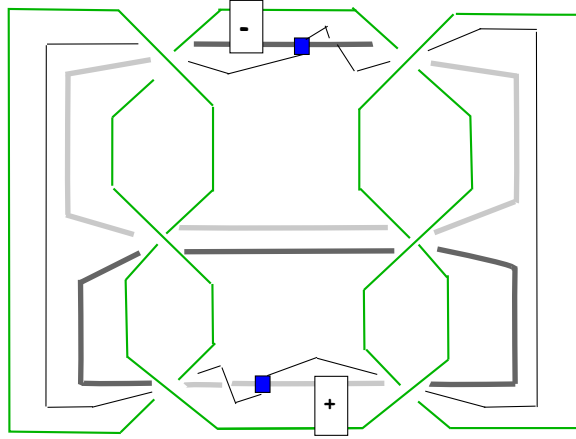
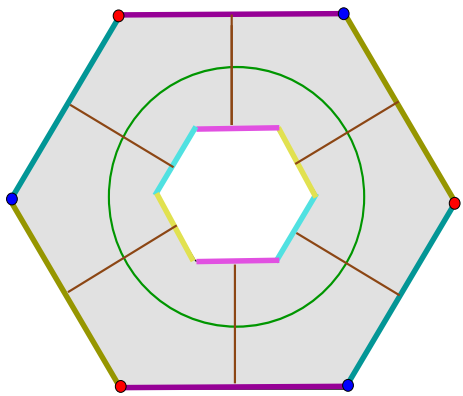


FIGURE 32.

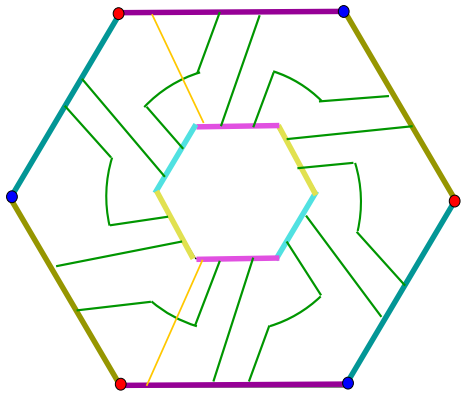
that Dehn twisting V_0 along curves in this torus produces links much simpler than the V_n (in fact mostly links obtained from $Q \cup V_0$ just by twisting Q , as described in the remarks before Theorem 5.1).

Here is a way to see a more complicated candidate for the torus T : Just as the trefoil knot contains a spanning Möbius band, the manifold M contains an interesting Klein bottle, the mapping cylinder of the six brown arcs in Figure 33(a). Other tori in M can be obtained from the swallow-follow torus by Dehn twisting it along the Klein bottle. (This must be done in the direction of the curve in the Klein bottle whose complement is orientable, in order for the operation to make sense). An example is shown in Figure 33(b): the union of the twelve green arcs is a circle that is preserved, with its orientation, by the monodromy, so its mapping cylinder is a torus T in M . We now verify that T is the torus we seek.

The yellow curve in Figure 33(b) is the original component V_0 ; it intersects T twice. Figure 34 shows (in red and blue) two parallel simple closed curves on T : As was the convention in Section 4 (see also Figure 17) imagine both the blue arc and the red arc lying in $F_\cup \times \{\frac{1}{2}\} \subset F_\cup \times I \subset M$. A green dot at the end of each arc is labeled \pm and represents in each case a vertical arc that ascends (resp. descends) to $F_\cup \times \{1\}$ (resp $F_\cup \times \{0\}$). The two ends of the blue arc (and similarly the two ends of the red arc) are then identified in M by the monodromy. The framing of these curves given by the normal direction to T is clearly the “blackboard framing” given by the figure, so Dehn twisting along T in the direction of these curves can be visualized by widening the blue and red arcs into bands, and then Dehn twisting along the bands. Finally, visibly identify the ends of the blue band



(a)



(b)

FIGURE 33.

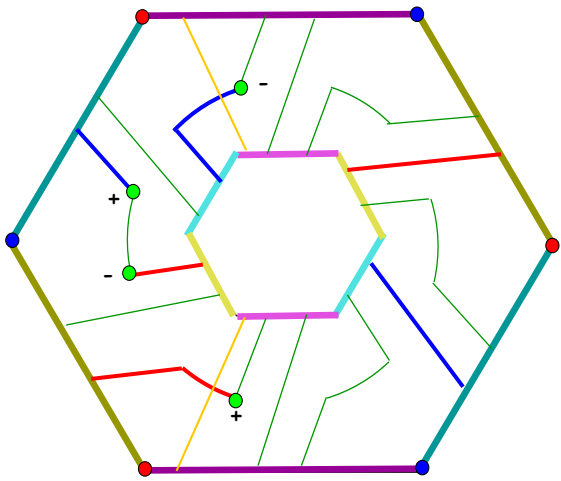


FIGURE 34.

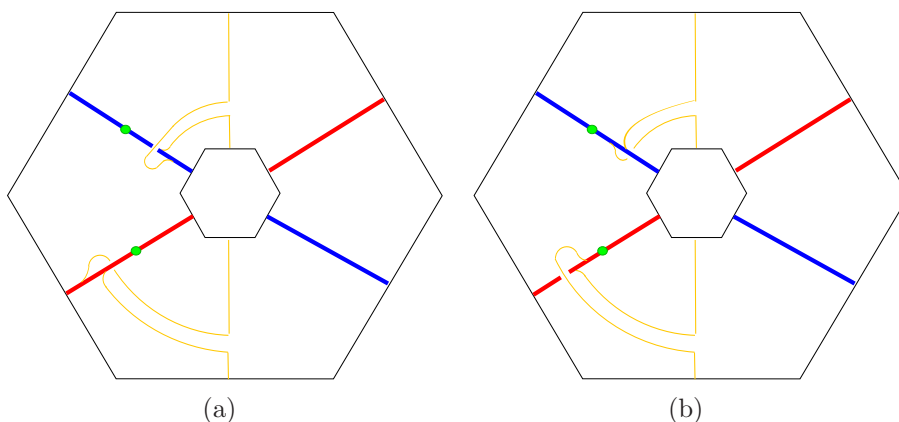


FIGURE 35.

(and the ends of the red band) by altering the monodromy near the central circle, as was done in Figure 9, to get red and blue annuli. The result is Figure 35(a), which uses train-track merging to show the direction of the Dehn twisting. The result is essentially identical to that shown in Figure 13 and can be made identical by flipping both red and blue annuli along their core curves (see Figure 35(b)). Why the colored annuli have framing ± 1 in S^3 (that is, before 0-surgery is done on Q to create M) is explained briefly in Section 4 via Figure 14.

This shows that constructing the links L_n described at the beginning of Section 1 is simple. The fact that all these L_n satisfy Weak Generalized Property R requires only the argument in [GST, Section 10]. However, the argument that each $L_n, n \geq 3$ is unlikely to satisfy Generalized Property R, on Andrews-Curtis grounds, still seems to require the full complexity of the original construction in [GST], with its roots in [Go].

REFERENCES

- [Go] R. Gompf, Killing the Akbulut-Kirby 4-sphere, with relevance to the Andrews-Curtis and Schoenflies problems *Topology* **30** (1991), 97–115.
- [GST] R. Gompf, M. Scharlemann and A. Thompson, Fibered knots and potential counterexamples to the Property 2R and Slice-Ribbon Conjectures, *Geometry and Topology* **14** (2010) 2305–2347.
- [GS] R. Gompf and A. Stipsicz, *4-Manifolds and Kirby Calculus*, Graduate Studies in Mathematics **20** American Mathematical Society, Providence, RI, 1999.
- [Ki1] R. Kirby, A calculus for framed links in S^3 *Invent. Math.* **45** (1978) 35–56.
- [Ki2] R. Kirby, Problems in Low-Dimensional Topology, in *Geometric Topology*, Edited by H. Kazez, AMS/IP Vol. 2, International Press, 1997.
- [L] Lickorish, W. B. R., A representation of orientable combinatorial 3-manifolds, *Ann. Math.* **76** (1962) 531–540.

- [ST] M. Scharlemann, A. Thompson, Surgery on knots in surface \times I, *ArXiv* 0807.0405
- [Z] E. Christopher Zeeman, Twisting spun knots, *Trans. Amer. Math. Soc.* **115** (1965) 471-495.

MARTIN SCHARLEMANN, MATHEMATICS DEPARTMENT, UNIVERSITY OF CALIFORNIA, SANTA BARBARA, CA USA
E-mail address: mgscharl@math.ucsb.edu

